Design, Synthesis, and Crystal Structure of Selective 2-Pyridone Tissue Factor VIIa Inhibitors

John J. Parlow,*,† Ravi G. Kurumbail,‡ Roderick A. Stegeman,‡ Anna M. Stevens,‡ William C. Stallings,‡ and Michael S. South†

Department of Medicinal and Combinatorial Chemistry, Pharmacia Corporation, 800 North Lindbergh Boulevard, St. Louis, Missouri 63167, and Structure and Computational Chemistry, Pharmacia Corporation, 700 Chesterfield Village Parkway, St. Louis, Missouri 63198

Received April 15, 2003

Targeted 2-pyridones were selected as tissue Factor VIIa inhibitors and prepared from 2,6-dibromopyridine via a multistep synthesis. A variety of chemical transformations, including regioselective nucleophilic addition, selective nitrogen alkylation, and a Suzuki coupling, afforded the targeted tissue Factor VIIa inhibitors. The pyridone core was selected as a replacement for the pyrazinone core of noncovalent tissue Factor VIIa inhibitors and designed such that their substitution pattern would occupy and interact with the S_1, S_2, and S_3 pockets of the tissue Factor VIIa enzyme. These compounds were tested in several serine protease enzyme assays involved in the coagulation cascade exhibiting modest activity on tissue Factor VIIa with excellent selectivity over thrombin and Factor Xa. Finally, an X-ray crystal structure of inhibitor **14a** bound to tissue Factor VIIa was obtained and will be described.

Introduction

Acute coronary syndromes (ACS) consisting of unstable angina, myocardial infarction, and sudden death are the most frequent cause of mortality in the United States and Western countries.[1] ACS is associated with acute thrombus formation, often as the result of a plaque rupture. Thrombosis also occurs in transient ischemic attack, stroke, peripheral occlusive arterial disease, deep vein thrombosis, pulmonary embolism, abrupt closure following angioplasty, and the disseminated intravascular coagulation associated with sepsis and certain cancers. Effective and safe antithrombotics are needed to combat these diseases. Most research has focused on thrombin and Factor Xa inhibitors as potentially valuable therapeutic agents for these diseases.[2] More recently, small molecule inhibitors of tissue Factor (TF) VIIa have been the point of much research effort because of their potential to inhibit the coagulation cascade while lessening the risk of bleeding side effects.[3] The extrinsic coagulation cascade is triggered by the binding of Factor VIIa to cell surface TF. This cascade is critical in normal hemostasis, but is also involved in the pathogenesis of various thrombotic diseases. Under normal conditions, TF expressed in the sub-endothelium of healthy blood vessels is not exposed to blood. However, in disease or injury, vessel wall or plaque TF is exposed and complexes with its cofactor Factor VIIa, leading to the activation of Factors IX and X. The complex of Factor Xa and Factor Va on a membrane surface converts prothrombin to thrombin, leading to fibrin formation, deposition, and subsequent thrombus formation.[4]

We previously reported the preparation of pyrazinone analogues as noncovalent tissue Factor VIIa inhibitors.[5]

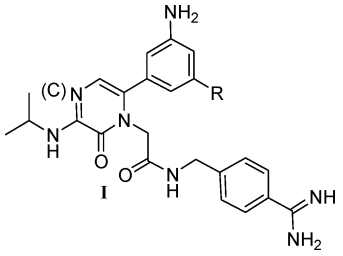

I

Figure 1. Pyrazinone core structure.

These pyrazinone compounds are active-site inhibitors for Factor VIIa exhibiting potency at the single-digit nanomolar level (IC_{50}) with excellent selectivity over thrombin (IIa) and Factor Xa. In an effort to increase the potency and influence the pharmocokinetic properties, other heterocyclic ring systems were evaluated. Depicted in Figure 1 is the lead pyrazinone core structure **I**. Focusing on the central ring, one of the exercises was to replace the nitrogen at the 4-position in the pyrazinone ring with carbon, resulting in a pyridone heterocycle as the core ring.[6] Other groups have disclosed the pyridone template in the design of human leukocyte elastase (HLC) inhibitors[7] and thrombin inhibitors.[8] We too were motivated by the attractiveness of the pyridone template and the fact that it has not been reported as a TF/VIIa inhibitor. Based on the structure−activity relationship established with the previously prepared pyrazinone analogues, two targeted pyridone analogues were selected for preparation. Herein, we describe their synthesis, biological activity, and X-ray crystal structure.

Results and Discussion

Several commercially available substituted pyridines were evaluated in terms of potential starting material for the synthesis. It was decided to proceed with the synthesis using readily available, inexpensive 2,6-

* To whom correspondence should be addressed. Phone: 314-274-3494. Fax 314-274-1621. e-mail: john.j.parlow@pfizer.com.
† Department of Medicinal and Combinatorial Chemistry.
‡ Structure and Computational Chemistry.

10.1021/jm0301686 CCC: $25.00
Published on Web 09/13/2003

Scheme 1[a]

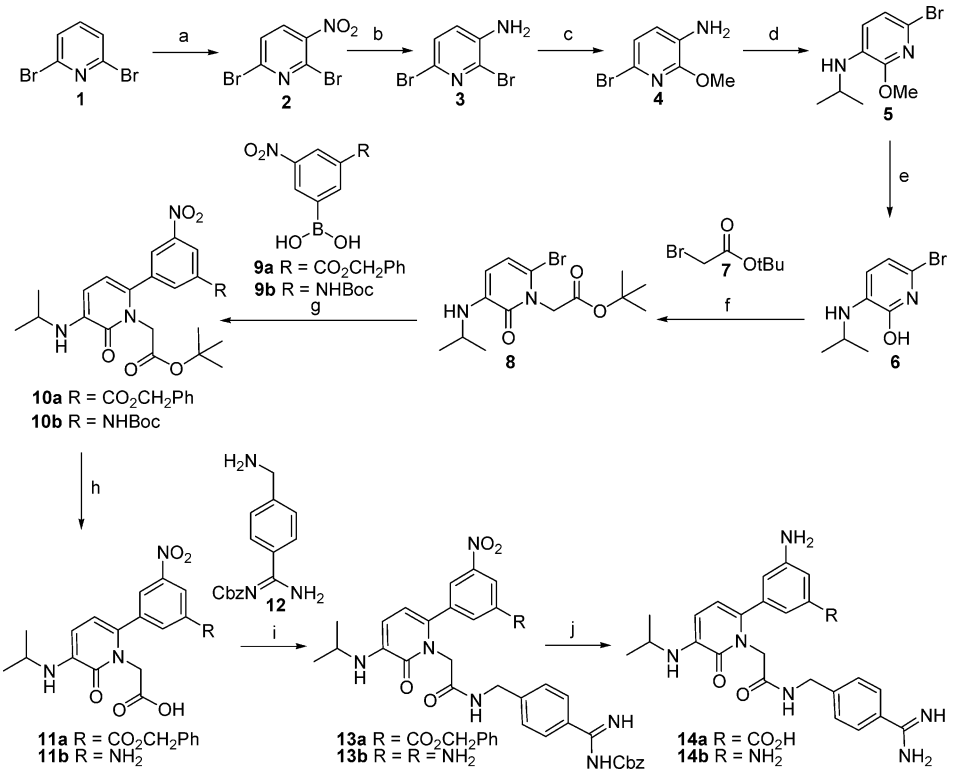

[a] Reagents: (a) NO_2BF_4, MeCN, reflux; (b) Fe, $MeCO_2H$, 80 °C; (c) NaOMe, dioxane, reflux; (d) $TiCl_4$, $NaCNBH_3$, Me_2CO, DCM; (e) BBr_3, DCM, −10 °C; (f) CaH_2, THF; (g) $Pd(PPh_3)_4$, Cs_2CO_3, dioxane, 80 °C; (h) 4 N HCl/dioxane; (i) HOBt, NMM, PS−CD, DCM/DMF, then PS-aldehyde and PS-polyamine; (j) H_2, Pd/C, MeOH.

dibromopyridine **1** as the starting material shown in Scheme 1. The dibromopyridine **1** was nitrated according to the literature procedure to afford 2,6-dibromo-3-nitropyridine **2**.[9] The nitro group was reduced with iron to afford the 3-amino-2,6-dibromopyridine **3**. Reacting the unsubstituted 3-amino-2,6-dibromopyridine **3** with sodium methoxide in dioxane at reflux afforded exclusively the desired regioisomer, 3-amino-6-bromo-2-methoxypyridine **4**. Several reductive amination conditions were surveyed. The preformation of the imine using titanium tetrachloride with acetone followed by reduction with sodium cyanoborohydride afforded cleanly the 6-bromo-2-methoxy-3-isopropylaminopyridine **5**.[10] The methoxy ether **5** was cleaved using boron tribromide to afford the hydroxypyridine **6**. Alkylation of the hydroxypyridine **6** with *tert*-butylbromoacetate **7** using calcium hydride as the base afforded a single isomer **8**. While alkylation could occur on either the nitrogen or the oxygen, only one regioisomer was isolated.[11] A Suzuki coupling of the *N*-alkylated bromopyridone **8** with the boronic acids **9** gave the biaryl compounds **10**. Selective hydrolysis of the *tert*-butyl ester with hydrochloric acid afforded the carboxylic acids **11**. The carboxylic acids **11** were coupled with benzyl amino[4-(aminomethyl)phenyl]methylenecarbamate **12** using polymer-bound carbodiimide, hydroxybenzotriazole, and *N*-methylmorpholine as base to afford the desired Cbz-protected products **13**. Concomitant deprotection of the Cbz (and benzyl ester with compound **13a**) and reduction of the nitro group was accomplished using hydrogen with palladium on carbon to afford the desired target compounds **14**.

Table 1. IC_{50} Values

	IC_{50} (uM)		
compd	VIIa	Xa	thrombin
14a	0.118	>30	>30
14b	0.052	>30	>30

The target compounds **14a** and **14b** were screened for potency on TF/VIIa and for other enzymes affecting coagulation to determine specificity (Table 1). Each enzyme assay consists of the specific enzyme and chromogenic substrate for that enzyme. Enzyme activity was determined by monitoring the increase in absorbance at 405 nm caused by the release of *p*-nitroaniline when the substrate is hydrolyzed. All compounds were assayed in duplicate at seven concentrations. Percent inhibition at each concentration was calculated from the OD_{405nm} value from the experimental and control sample. IC_{50} values were calculated from a four-parameter logistic regression equation. For each compound the individual IC_{50} values were within 10% of each other. The reported IC_{50} represents an average of the duplicates. Reported are the inhibition data as IC_{50} values for TF/VIIa, Factor Xa, and thrombin. Compounds **14a** and **14b** are both active against TF/VIIa with an IC_{50} of 118 nM and 52 nM, respectively. Both compounds are selective over thrombin and Factor Xa exhibiting no activity at 30 μM. However, both pyridones **14a** and **14b** are approximately 5× less potent against TF/VIIa than their corresponding pyrazinone analogues.[5]

The crystal structure of compound **14a** bound to TF/VIIa is shown in Figure 2. The benzamidine moiety of the pyridone inhibitor forms an ion-pair with the

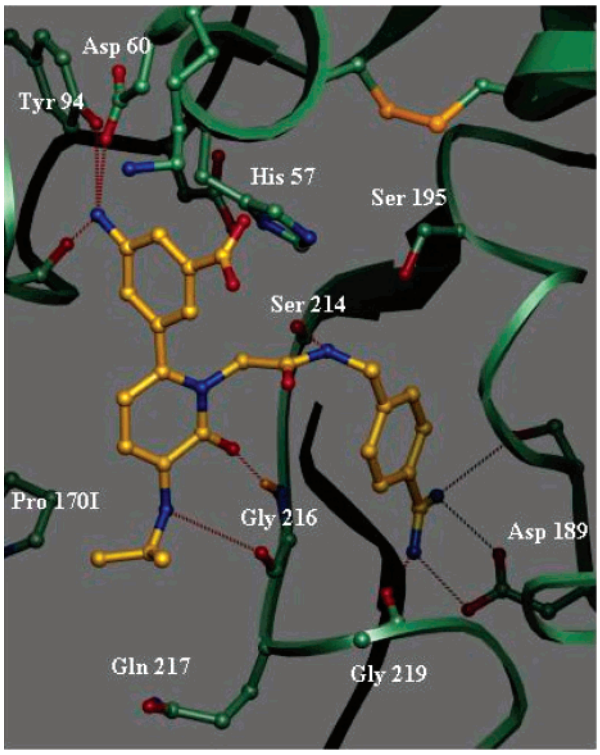

Figure 2. Crystal structure of pyridone inhibitor **14a** bound in the active site of TF/VIIa comlex. The structure was refined to an R_{free} of 27.5% at 2.2 Å resolution ($R_{crystal}$:21.3%). Some of the key side chains of Factor VIIa are displayed (C: green, N: dark blue, O: red, S: yellow and H: orange). The inhibitor is represented with carbon, nitrogen, and oxygen atoms displayed in gold, blue, and red, respectively. The hydrogen bonds formed by the inhibitor are shown in dotted (magenta) lines.

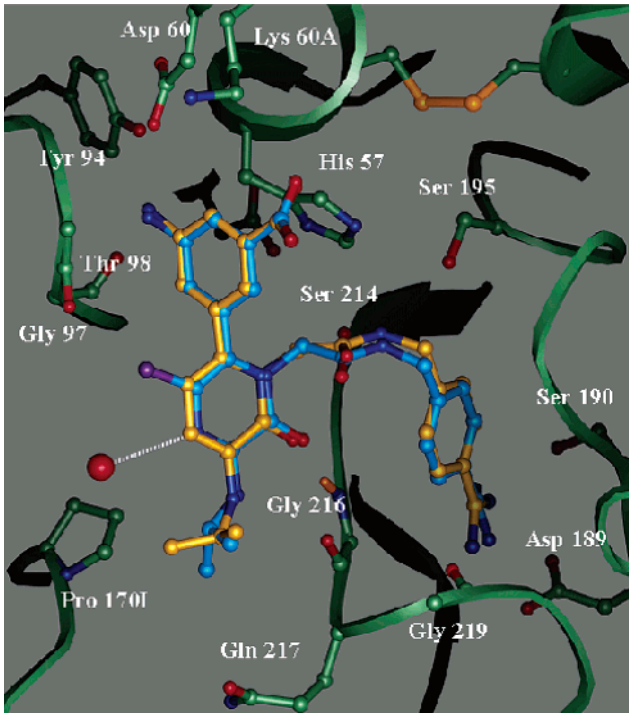

Figure 3. Overlap of the crystal structures of compound **14a** (multiccolored as shown in Figure 2) and a closely related pyrazinone (cyan) inhibitor. The protein atoms of the pyrazinone complex are not shown for clarity. For superposition of the two structures, only the α-carbon atoms of the catalytic domain of VIIa were used. The second nitrogen atom of the pyrazinone inhibitor forms an additional hydrogen bond to a bound solvent molecule (red sphere).

carboxylate of Asp 189 as observed in the structures of pyrazinone complexes with TF/VIIa.[30,31] The pyridone carbonyl oxygen accepts a hydrogen bond (3.0 Å) from the amide nitrogen of Gly 216. The amide nitrogen of the glycine linker (between benzamidine and the pyridone core) forms a hydrogen bond to the carbonyl oxygen of Ser 214 (3.3 Å). Moreover, the 3-amino group on the pyridone core interacts with the carbonyl oxygen of Gly 216 (3.2 Å). The *m*-amino group on the phenyl ring at P_2 forms a four-centered H-bond network with the main chain oxygen of Thr 98 and with the side chains of Tyr 94 and Asp 60.

Figure 3 shows the overlap of compound **14a** with a closely related pyrazinone inhibitor.[5] As expected, most of the functional groups of the pyrazinone and pyridone inhibitors superimpose well in their bound conformations. The binding sites and the dihedral angles are well conserved between the pyridone and the pyrazinone inhibitors. Small differences are found in the conformations of the isopropyl groups at P_3. There are two key differences between the two inhibitors: (a) presence of a chlorine atom on the pyrazinone ring, (b) replacement of the second nitrogen atom by a carbon in the pyridone. The chlorine atom of the pyrazinone inhibitor is within van der Waals distance (3.1 A) of the carbonyl oxygen of Gly 97 (Figure 3). This might contribute to the enhanced potency of the pyrazinone inhibitor for TF/VIIa (~5×). The second nitrogen atom (4-position) of the pyrazinone ring forms a hydrogen bond to a bound water molecule (3.2 Å). A similar solvent molecule is observed in most of the pyrazinone structures that have been determined. The bound solvent molecule appears to be trapped between the side chain of Pro 170I and the pyrazinone inhibitor. Thus, compared to pyrazinone, the pyridone inhibitor forms one less hydrogen bond in the active site of VIIa. While it is true that the extra hydrogen bond in the case of pyrazinone inhibitor is with a bound solvent molecule and is relatively weak, it nevertheless could account for a slight increase in the binding affinity of this class of inhibitors relative to pyridones. Moreover, the extra nitrogen atom in the pyrazinone ring (in comparison to pyridone core) could also lead to better hydrogen bonding interactions of the core with the atoms of VIIa. These factors together could explain why the pyridones are slightly weaker inhibitors of VIIa compared to the pyrazinones.

In summary, targeted pyridones were successfully prepared via multistep synthesis using various transformations and regioselective additions with a pyridine nucleus to afford novel pyridone derivatives. The analogues were tested against TF/VIIa but were less potent than their corresponding pyrazinone analogues. The X-ray crystal structure of targeted pyridone **14a** was obtained and compared with a closely related pyrazinone inhibitor, suggesting that additional hydrogen bonding and van der Waals interactions may be responsible for the enhanced potency of the pyrazinone inhibitor. With no improved potency and a lack of favorable pharmacokinetics, further syntheses using the pyridone as the core ring were not pursued.

Experimental Section

Assays for Biological Activity. Recombinant soluble TF, consisting of amino acids 1−219 of the mature protein sequence was expressed in *E. coli* and purified using a Mono Q Sepharose FPLC. Recombinant human VIIa was purchased from American Diagnostica (Greenwich, CT) and chromogenic substrate *N*-methylsulfonyl-D-phe-gly-arg-*p*-nitroaniline was prepared by American Peptide Company, Inc. (Sunnyvale, CA). Factor Xa was obtained from Enzyme Research Laboratories (South Bend, IN), thrombin from Calbiochem (La Jolla, CA), and trypsin and L-BAPNA from Sigma (St. Louis, MO). The chromogenic substrates S-2765 and S-2238 were purchased from Chromogenix (Sweden).

TF−VIIa Assay. Recombinant soluble tissue factor (100 nM) and recombinant human Factor VIIa (2 nM) were added to a 96-well assay plate containing 0.4 mM of the substrate, *N*-methylsulfonyl-D-phe-gly-arg-*p*-nitroaniline and either inhibitor or buffer (5 mM $CaCl_2$, 50 mM Tris-HCl, pH 8.0, 100 mM NaCl, 0.1% BSA). The reaction, in a final volume of 100 mL, was measured immediately at 405 nm to determine background absorbance. The plate was incubated at room temperature for 60 min, at which time the rate of hydrolysis of the substrate was measured by monitoring the reaction at 405 nm for the release of *p*-nitroaniline. All compounds were assayed in duplicate at seven concentrations. Percent inhibition at each concentration was calculated from OD_{405nm} value from the experimental and control sample. IC_{50} values were calculated from a four-parameter logistic regression equation. For each compound the individual IC_{50} values were within 10% of each other. The reported IC_{50} represents an average of the duplicates.

Factor Xa Assay. Human Factor Xa (0.3 nM) and *N*-α-benzyloxycarbonyl-D-arginyl-L-glycyl-L-arginine-*p*-nitroaniline dihydrochloride (S-2765) (0.15 mM) were added to a 96-well assay plate containing either inhibitor or buffer (50 mM Tris-HCl, pH 8.0, 100 mM NaCl, 0.1% BSA). The reaction, in a final volume of 100 μL, was measured immediately at 405 nm to determine background absorbance. The plate was incubated at room temperature for 60 min, at which time the rate of hydrolysis of the substrate was measured by monitoring the reaction at 405 nm for the release of *p*-nitroaniline. All compounds were assayed in duplicate at seven concentrations. Percent inhibition at each concentration was calculated from OD_{405nm} value from the experimental and control sample. IC_{50} values were calculated from a four-parameter logistic regression equation. For each compound the individual IC_{50} values were within 10% of each other. The reported IC_{50} represents an average of the duplicates.

Thrombin Assay. Human thrombin (0.28 nM) and *H*-D-phenylalanyl-L-pipecolyl-L-arginine-*p*-nitroaniline dihydrochloride (0.06 mM) were added to a 96-well assay plate containing either inhibitor or buffer (50 mM Tris-HCl, pH 8.0, 100 mM NaCl, 0.1% BSA). The reaction, in a final volume of 100 mL, was measured immediately at 405 nm to determine background absorbance. The plate was incubated at room temperature for 60 min, at which time the rate of hydrolysis of the substrate was measured by monitoring the reaction at 405 nm for the release of *p*-nitroaniline. All compounds were assayed in duplicate at seven concentrations. Percent inhibition at each concentration was calculated from OD_{405nm} value from the experimental and control sample. IC_{50} values were calculated from a four-parameter logistic regression equation. For each compound the individual IC_{50} values were within 10% of each other. The reported IC_{50} represents an average of the duplicates.

Chemistry. General. ^1H and ^{13}C NMR spectra were recorded using a 300 and 400 MHz NMR spectrometer. Sample purities were determined by HPLC analysis equipped with a mass spec detector using a C18 3.5 um 30 × 2.1 mm column, eluting with a gradient system of 5/95 to 95/5 acetonitrile/water with a buffer consisting of 0.1% TFA over 4.5 min at 1 mL/min and detected by UV at 254 and 210 nm using a diode array detector. Column chromatography was performed on a preparative liquid chromatography instrument using silica gel columns and on a HPLC system using a 15um 100A, C18 column (25 mm ID × 100 mm L). Reported yields are not optimized, with emphasis on purity of products rather than quantity.

3-Amino-2,6-dibromopyridine (3). The 2,6-dibromo-3-nitropyridine **2** (6.8 g, 24.3 mmol) was stirred in glacial acetic acid. Powdered iron (6.7 g, 119 mmol) was added, and the solution was heated to 80 °C with vigorous stirring. The solution was stirred at 80 °C for 15 min at which point the iron had turned gray. The reaction mixture was filtered through Celite, and the solid was washed with diethyl ether and ethyl acetate. The resultant organic layer was washed with water and brine, dried over magnesium sulfate, and filtered. The solvent was removed to afford the crude product. The product was purified by column chromatography (20% ethyl acetate−hexane) to afford 5.26 g (87%) of a white solid of product **3**; ^1H NMR ppm (deuteriochloroform): 3.89 (s, 2H), 6.89 (d, 1H, J = 8.4 Hz), 7.10 (d, 1H, J = 8.4 Hz); ^{13}C NMR ppm (deuteriochloroform): 124.8, 125.7, 126.9, 127.7, 141.8; HPLC purity (retention time): >99% (2.95 min); HRMS calcd for $C_4H_4Br_2N_2$ ($M^+ + H$) 252.8799, found 252.8779.

6-Bromo-2-methoxypyridin-3-amine (4). A solution of 3-amino-2,6-dibromopyridine **3** (10.4 g, 41.5 mmol) and sodium methoxide (15.7 g, 290 mmol) in dioxane was heated to reflux for 48 h. The brown reaction was allowed to cool to room temperature and diluted with a saturated solution of ammonium chloride. The solution was extracted with diethyl ether, and the organic layer was washed with water, brine, dried over magnesium sulfate, and filtered. The solvent was removed by evaporation to afford the crude product. The product was purified by column chromatography (20% ethyl acetate−hexane) to afford 7.1 g (84%) of a red solid of product **4**; ^1H NMR ppm (deuteriochloroform): 3.94 (s, 3H), 6.71 (d, 1H, J = 6.0 Hz), 6.83 (d, 1H, J = 6.0 Hz); ^{13}C NMR ppm (deuteriochloroform): 67.2, 120.4, 122.5, 124.1, 130.3, 152.4; HPLC purity (retention time): 94% (2.92 min); HRMS calcd for $C_6H_7Br_1N_2O$ ($M^+ + H$) 204.9800, found 204.9769.

6-Bromo-*N*-isopropyl-2-methoxypyridin-3-amine (5). A solution of 1 M titanium tetrachloride in dichloromethane (37 mL, 37 mmol) was added to a solution of 6-bromo-2-methoxypyridin-3-amine **4** (6.8 g, 33.6 mmol) and acetone (3.3 mL, 44.9 mmol) in dichloromethane. After the mixture was stirred at room temperature for 3 h, sodium cyanoborohydride (6.3 g, 100 mmol) was added and the solution stirred at room temperature for 14 h. The solution was diluted with diethyl ether and water. The organic layer was washed with brine, dried over magnesium sulfate, and filtered. The solvent was removed by evaporation to afford the crude product. The product was purified by column chromatography (5% ethyl acetate−hexane) to afford 5.7 g (69%) of a red oil of product **5**; ^1H NMR ppm (deuteriochloroform): 1.20 (d, 6H), 3.51 (septet, 1H), 3.95 (s, 3H), 6.62 (d, 1H, J = 6.0 Hz), 6.88 (d, 1H, J = 6.0 Hz); HPLC purity (retention time): 95% (3.97 min); HRMS calcd for $C_9H_{13}Br_1N_2O$ ($M^+ + H$) 245.0289, found 245.0240.

6-Bromo-3-(isopropylamino)pyridin-2-ol (6). A solution of 1 M boron tribromide in dichloromethane (46.0 mL, 46 mmol) was added to a solution of 6-bromo-*N*-isopropyl-2-methoxypyridin-3-amine **5** (5.6 g, 0.23 mmol) in dichloromethane at −10 °C. The solution warmed to room temperature and stirred for 16 h. The reaction mixture was diluted with water, neutralized with a saturated sodium bicarbonate solution, and extracted with diethyl ether. The organic layer was washed with water and brine, dried over magnesium sulfate, and filtered. The solvent was removed by evaporation to afford the crude product. The product was purified by column chromatography (40% ethyl acetate−hexane) to afford 4.12 g (78%) of a white solid of product **6**; ^1H NMR ppm (deuteriochloroform): 1.22 (d, 6H), 3.49 (septet, 1H), 6.20 (d, 1H), 6.88 (d, 1H); ^{13}C NMR ppm (deuteriochloroform): 22.3, 44.1, 110.0, 128.6, 132.2, 136.4, 160.0; HPLC purity (retention time): 94% (2.45 min); HRMS calcd for $C_8H_{11}Br_1N_2O$ ($M^+ + H$) 231.0133, found 231.0130.

***tert*-Butyl [6-Bromo-3-(isopropylamino)-2-oxopyridin-1(2*H*)-yl]acetate (8).** A suspension of calcium hydride (1.7 g, 40.3 mmol) in tetrahydrofuran was added to 6-bromo-3-(isopropylamino)pyridin-2-ol **6** (4.2 g, 18 mmol) in tetrahydrofuran dropwise via an addition funnel. The resulting suspension was heated to reflux for 30 min. To the mixture was then added a solution of *tert*-butyl bromoacetate **7** (2.9 mL, 19.6 mmol) in tetrahydrofuran (2.3 M). Refluxing of the mixture was continued for 18 h. The reaction mixture was allowed to cool to room temperature and quenched with an ice−water mixture. The aqueous layer was extracted with diethyl ether. The organic layer was washed with water and brine, dried over magnesium sulfate, and filtered. The solvent was removed by evaporation to afford the crude product. The product was purified by column chromatography (10% ethyl acetate−hexane) to afford 4.1 g (66%) of a white solid of product **8**; ^{1}H NMR ppm (deuteriochloroform): 1.08 (H20,H15) (d, 6H, J = 6.4 Hz), 1.37 (H11,18,19) (s, 9H), 3.42 (H14) (septet, 1H, J = 6.4 Hz, 8.4 Hz), 4.81 (H7) (s, 2H), 5.05 (NH13) (d, 1H, J = 8.4 Hz), 6.13 (H4) (d, 1H, J = 7.9 Hz), 6.46 (H5) (d, 1H, J = 7.9 Hz); ^{13}C NMR ppm (DMSO): 22.3 (C15,C20), 28.2 (C11,18,-19), 43.6 (C14), 50.7 (C7), 82.5 (C10), 107.0 (C4), 111.8 (C5), 136.8 (C3), 158.4 (C2), 167.1 (C8); HPLC purity (retention time): 98% (4.63 min); HRMS calcd for $C_{14}H_{21}Br_1N_2O_3$ (M^+ + H) 345.0814, found 345.0827.

Benzyl 3-[1-(2-*tert*-Butoxy-2-oxoethyl)-5-(isopropylamino)-6-oxo-1,6-dihydropyridin-2-yl]-5-nitrobenzoate (10a). Tetrakis(triphenylphosphine)palladium(0) (0.20 g, 0.17 mmol) was added to a solution of compound **8** (0.60 g, 1.7 mmol), boronic acid **9a** (0.68 g, 2.3 mmol), and cesium carbonate (2.2 g, 6.7 mmol) in 18 mL of anhydrous dioxane. The resulting mixture stirred for at 80 °C for 16 h. The reaction mixture was allowed to cool to room temperature and was diluted with water and extracted with diethyl ether. The organic layer was washed with water and brine, dried over magnesium sulfate, and filtered. The solvent was removed by evaporation to afford the crude product. The product was purified by column chromatography (25% ethyl acetate−hexane) to afford 0.70 g (78%) of a red solid of product **10a**; ^{1}H NMR ppm (deuteriochloroform): 1.24 (d, 6H,), 1.39 (s, 9H), 3.57 (septet, 1H), 4.41 (s, 2H), 5.39 (s, 2H), 6.14 (d, 1H), 6.40 (d, 1H), 7.40 (m, 6H), 8.35 (m, 1H), 8.42 (m, 1H), 8.85 (m, 1H); HPLC purity (retention time): >99% (5.70 min); HRMS calcd for $C_{28}H_{31}N_3O_7$ (M^+ + H) 522.2240, found 522.2242.

***tert*-Butyl [6-{3-[(*tert*-Butoxycarbonyl)amino]-5-nitrophenyl}-3-(isopropylamino)-2-oxopyridin-1(2*H*)-yl]acetate (10b).** Following the same procedure described for **10a**, tetrakis(triphenylphosphine)palladium(0) (0.33 g, 0.28 mmol), compound **8** (1.0 g, 2.9 mmol), boronic acid **9b** (1.3 g, 4.6 mmol), and cesium carbonate (3.7 g, 11.3 mmol) were used to give 0.57 g (39%) of an orange solid of product **10b**; ^{1}H NMR ppm (deuteriochloroform): 1.24 (d, 6H,), 1.40 (s, 9H), 1.49 (s, 9H), 3.67 (septet, 1H), 4.43 (s, 2H), 6.14 (m, 2H), 7.20 (m, 1H), 7.64 (m, 1H), 7.82 (m, 6H), 8.35 (m, 1H); HPLC purity (retention time): 96% (5.37 min); LRMS for $C_{25}H_{34}N_4O_7$ (ES, *m*/*z*) 503 (M^+ + H).

[6-{3-[(Benzyloxy)carbonyl]-5-nitrophenyl}-3-(isopropylamino)-2-oxopyridin-1(2*H*)-yl]acetic Acid (11a). The *tert*-butyl ester **10a** (0.60 g, 1.1 mmol) was dissolved into 4 N hydrochloric acid in dioxane and stirred at room temperature for 22 h. The solvent was removed under a stream of nitrogen to afford a red gum of product **11a** [Note: Using heat during the evaporation of the solvent in the workup of acid **11a** led to decarboxylation to afford the *N*-methyl derivative (benzyl 3-[5-(isopropylamino)-1-methyl-6-oxo-1,6-dihydropyridin-2-yl]-5-nitrobenzoate). As a result, evaporation of the solvent was conducted using a stream of nitrogen.]; ^{1}H NMR ppm (deuteriochloroform): 1.53 (d, 6H,), 3.86 (septet, 1H), 4.55 (s, 2H), 5.39 (s, 2H), 6.42 (d, 1H), 7.39 (m, 5H), 8.29 (d, 1H), 8.37 (m, 1H), 8.44 (m, 1H), 8.94 (m, 1H); HPLC purity (retention time): 78% (4.67 min); HRMS calcd for $C_{24}H_{23}N_3O_7$ (M^+ + H) 466.1614, found 466.1625.

[6-(3-Amino-5-nitrophenyl)-3-(isopropylamino)-2-oxopyridin-1(2*H*)-yl]acetic Acid (11b). Following the same procedure described for **11a**, *tert*-butyl ester **10b** (0.50 g, 0.10 mmol), was used to afford a yellow solid of product **11b**; ^{1}H NMR ppm (deuteriomethanol): 1.38 (d, 6H), 3.87 (septet, 1H), 4.63 (s, 2H), 6.48 (d, 1H), 7.42 (m, 1H), 7.82 (m, 2H), 7.82 (m, 1H), 8.00 (m, 1H); HPLC purity (retention time): 90% (2.72 min); HRMS calcd for $C_{16}H_{18}N_4O_5$ (M^+ + H) 347.1350, found 347.1334.

Benzyl 3-[1-(2-{[4-((*E*)-Amino{[(benzyloxy)carbonyl]-imino}methyl)benzyl]amino}-2-oxoethyl)-5-(isopropylamino)-6-oxo-1,6-dihydropyridin-2-yl]-5-nitrobenzoate (13a). Polystyrene-carbodiimide (2.3 g, 2.3 mmol) (1.00 mmol/g) was added to a slurry of the acid **11a** (0.53 g, 1.1 mmol), 1-hydroxybenzotriazole (0.16 g, 0.71 mmol), benzyl amino[4-(aminomethyl)phenyl]methylcarbamate **12** (0.44 g, 1.3 mmol), and *N*-methylmorpholine (1.3 mL, 11.8 mmol) in a dichloromethane−*N*,*N*-dimethylformamide (3:1) solution, and the suspension was agitated for 13 h. Upon completion of the reaction, the polyamine resin (2.81 mmol/g) (5.6 mmol) and polymer-bound aldehyde (2.3 mmol/g) (2.30 mmol) were added, and the suspension was agitated for 1 h. The solution was filtered, and the polymer was rinsed with *N*,*N*-dimethylformamide and dichloromethane until no more UV activity was seen in the dichloromethane washing. The solvent was removed by evaporation to afford the crude product. The product was purified by reverse-phase chromatography to afford 0.73 g (87%) of an orange solid of product **13a**; ^{1}H NMR ppm (deuterioacetone): 1.19 (d, 6H,), 3.48 (septet, 1H), 4.41 (d, 2H), 4.63 (s, 2H), 5.18 (s, 2H), 5.48 (s, 2H), 6.30 (m, 2H), 7.40 (m, 11H), 7.99 (d, 1H), 8.18 (bt, 1H), 8.58 (m, 1H), 8.68 (m, 1H), 8.78 (m, 1H); HPLC purity (retention time): 90% (4.50 min); HRMS calcd for $C_{40}H_{38}N_6O_8$ (M^+ + H) 731.2829, found 731.2853.

Benzyl (1*E*)-Amino{4-[({[6-(3-amino-5-nitrophenyl)-3-(isopropylamino)-2-oxopyridin-1(2*H*)-yl]acetyl}amino)-methyl]phenyl}methylidenecarbamate (13b). Following the same procedure described for **13a**, polystyrene-carbodiimide (2.0 g, 2.0 mmol) (1.00 mmol/g), the acid **11b** (0.34 g, 3.4 mmol), 1-hydroxybenzotriazole (0.14 g, 1.0 mmol), benzyl amino[4-(aminomethyl)phenyl]methylcarbamate **12** (0.38 g, 1.2 mmol), and *N*-methylmorpholine (1.1 mL, 10 mmol) was used to afford 0.24 g (39%) of a yellow solid of product **13b**; ^{1}H NMR ppm (deuteriodimethylformamide): 1.36 (d, 6H), 3.70 (septet, 1H), 4.56 (d, 2H), 4.75 (s, 2H), 5.33 (s, 2H), 6.25 (d, 1H), 6.43 (d, 1H), 7.53 (m, 8H), 8.06 (m, 4H), 8.57 (bt, 1H), 11.16 (bs, 1H); HPLC purity (retention time): 80% (3.41 min); HRMS calcd for $C_{32}H_{33}N_7O_6$ (M^+ + H) 612.2565, found 612.2521.

3-Amino-5-[1-[2-({4-[amino(imino)methyl]benzyl}-amino)-2-oxoethyl]-5-(isopropylamino)-6-oxo-1,6-dihydropyridin-2-yl]benzoic Acid (14a). A catalytic amount of palladium on carbon (10%) in methanol was added to compound **13a** (0.33 g, 0.45 mmol) in methanol, and the mixture was stirred under a balloon of hydrogen at room temperature for 6 h. The mixture was filtered through Celite, and the solvent was evaporated to afford the product. The product was purified by reverse-phase chromatography to afford 0.28 g (88%) of a yellow solid of product **14a**; ^{1}H NMR ppm (deuteriomethanol): 1.26 (d, 6H), 3.63 (septet, 1H), 4.44 (d, 2H), 4.65 (d, 2H), 6.27 (dd, 1H), 6.78 (dd, 1H), 7.62 (m, 9H); HPLC purity (retention time): >99% (2.39 min); HRMS calcd for $C_{25}H_{28}N_6O_4$ (M^+ + H) 477.2250, found 477.2253.

***N*-{4-[Amino(imino)methyl]benzyl}-2-[6-(3,5-diaminophenyl)-3-(isopropylamino)-2-oxopyridin-1(2*H*)-yl]acetamide (14b).** A catalytic amount of palladium on carbon (10%) in methanol was added to compound **13b** (0.20 g, 0.32 mmol) in methanol, and the mixture was stirred under a balloon of hydrogen at room temperature for 12 h. The mixture was filtered through Celite, and the solvent was evaporated to afford the product. The product was purified by reverse-phase chromatography to afford 0.24 g (39%) of a brown solid of product **14b**; ^{1}H NMR ppm (deuteriomethanol): 1.26 (d, 6H), 3.63 (septet, 1H), 4.44 (d, 2H), 4.65 (d, 2H), 6.27 (dd, 1H), 6.78 (dd, 1H), 7.62 (m, 9H); HPLC purity (retention time): >99% (2.39 min); HRMS calcd for $C_{24}H_{29}N_7O_2$ (M^+ + H) 448.2456, found 448.2447.

Acknowledgment. The authors thank Rhonda M. Lachance for the biological evaluation and Dr. Huey Shieh for some of the early crystallographic refinements of the TF/VIIa structure. Diffraction data for the TF/VIIa complex with the different inhibitors were collected at beamline 17-ID in the facilities of the Industrial Macromolecular Crystallography Association Collaborative Access Team (IMCA-CAT) at the Advanced Photon Source. IMCA-CAT facilities are supported by the corporate members of the IMCA and through a contract with Illinois Institute of Technology (IIT), executed through the IIT's Center for Synchrotron Radiation Research and Instrumentation. Use of the Advanced Photon Source was supported by the U.S. Department of Energy, Basic Energy Sciences, Office of Science, under Contract No. W-31-109-Eng-38.

Supporting Information Available: Spectral characterization data for all compounds. This material is available free of charge via the Internet at http://pubs.acs.org.

References

(1) Braunwald, E.; Califf, R. M.; Cannon, C. P.; Fox, K. A.; Fuster, V.; Gibler, W. B.; Harrington, R. A.; King, S. B.; Kleiman, N. S.; Theroux, P.; Topol, E. J.; Van de Werf, F.; White, H. D.; Willerson, J. T. Redefining medical treatment in the management of unstable angina. *Am. J. Med.* **2000**, *108*, 41−53.

(2) For reviews see: (a) Sanderson, P. E. J. Anticoagulants: Inhibitors of thrombin and Factor Xa. *Annu. Rep. Med. Chem.* **2001**, *36*, 79−88. (b) Betz, A. Recent advances in Factor Xa inhibitors. *Expert Opin. Ther. Pat.* **2001**, *11*, 1007−1017. (c) Zhu, B. Y.; Scarborough, R. M. Factor Xa inhibitors: Recent advances in anticoagulant agents. *Annu. Rep. Med. Chem.* **2000**, *35*, 83−102. (d) Vacca, J. P. New advances in the discovery of thrombin and Factor Xa inhibitors. *Curr. Opin. Chem. Biol.* **2000**, *4*, 394−400. (e) Sanderson, P. E. J. Small, noncovalent serine protease inhibitors. *Med. Res. Rev.* **1999**, *19*, 179−197. (f) Fevig, J. M.; Wexler, R. R. Anticoagulants: Thrombin and Factor Xa inhibitors. *Annu. Rep. Med. Chem.* **1999**, *34*, 81−100. (g) Ewing, W. R.; Pauls, H. W.; Spada, A. P. Progress in the design of inhibitors of coagulation Factor Xa. *Drug. Future* **1999**, *24*, 771−787.

(3) For reviews see and references therein: (a) Robinson, L. A.; Saiah, **E.** M. K. Anticoagulants: inhibitors of the Factor VIIa/tissue factor pathway. *Annu. Rep. Med. Chem.* **2002**, *37*, 85−94. (b) Girard, T. J.; Nicholson, N. S. The role of tissue factor/Factor VIIa in the pathophysiology of acute thrombotic formation. *Curr. Opin. Pharmacol.* **2001**, *1*, 159−163.

(4) (a) Houston, D. S. Tissue factor − a therapeutic target for thrombotic disorders. *Expert Opin. Ther. Targets* **2002**, *6*, 159−174. (b) Golino, P. The inhibitors of the tissue factor: Factor VII pathway. *Thromb. Res.* **2002**, *106*, V257−V265. (c) Bajaj, M. S.; Birktoft, J. J.; Steer, S. A.; Bajaj, S. P. Structure and biology of tissue factor pathway inhibitor. *Thromb. Haemost.* **2001**, *86*, 959−972. (d) Kaiser, B.; Hoppensteadt, D. A.; Fareed, J. Tissue factor pathway inhibitor: an update of potential implications in the treatment of cardiovascular disorders. *Expert Opin. Invest. Drugs* **2001**, *10*, 1925−1935. (e) Kirchhofer, D.; Nemerson, Y. Initiation of blood coagulation: the tissue factor/Factor VIIa complex. *Curr. Opin. Chem. Biotechnol.* **1996**, *7*, 386−391. (f) Girard, T. J. Tissue Factor Pathway Inhibitor. In *New Therapeutic Agents in Thrombosis and Thrombolysis*; Sasahara, A. A, Loscalzo, J., Eds.; Marcel Dekker: New York, 1998.

(5) (a) South, M. S.; Case, B. L.; Wood, R. S.; Jones, D. E.; Hayes, M. J.; Girard, T. J.; Lachance, R. M.; Nicholson, N. S.; Clare, M.; Stevens, A. M.; Stegeman, R. A.; Stallings, W. C.; Kurumbail, R. G.; Parlow, J. J. Structure-based drug design of pyrazinone antithrombotics as selective inhibitors of the tissue Factor VIIa complex. *Bioorg. Med. Chem. Lett.* **2003**, *13*, 2319−2325. (b) Parlow, J. J.; Case, B. L.; Dice, T. A.; Hayes, M. J.; Jones, D. E.; Neumann, W. L.; Wood, R. S.; Lachance, R. M.; Girard, T. J.; Nicholson, N. S.; Clare, M.; Stegeman, R. A.; Stevens, A. M.; Stallings, W. C.; Kurumbail, R. G.; South, M. S. Design, parallel synthesis, and crystal structures of pyrazinone antithrombotics as selective inhibitors of the tissue Factor VIIa complex. *J. Med. Chem.* **2003**, *46*, 4050−4062.

(6) South, M. S.; Zeng, Q.; Rueppel, M. L. Preparation of (heteroaryl)pyridones as coagulation cascade serine protease inhibitors. WO 0069826, 2000.

(7) (a) Damewood, J. R., Jr.; Edwards, P. D.; Feeney, S.; Gomes, B. C.; Steelman, G. B.; Tuthill, P. A.; Williams, J. C.; Warner, P.; Woolson, S. A.; Wolanin, D. J.; Veale, C. A. Nonpeptidic inhibitors of human leukocyte elastase. 2. Design, synthesis, and in vitro activity of a series of 3-amino-6-arylopyridin-2-one trifluoromethyl ketones. *J. Med. Chem.* **1994**, *37*, 3303−3312. (b) Warner, P.; Green, R. C.; Gomes, B.; Strimpler, A. M. Nonpeptidic inhibitors of human leukocyte elastase. 1. The design and synthesis of pyridone-containing inhibitors. *J. Med. Chem.* **1994**, *37*, 3090−3099. (c) Brown, F. K. J.; Andisik, D. W.; Bernstein, P. R.; Bryant, C. B.; Ceccarelli, C.; Damewood, J. R., Jr.; Edwards, P. D.; Earley, R. A.; Feeney, S.; Green, R. C.; Gomes, B.; Kosmider, B. J.; Krell, R. D.; Shaw, A.; Steelman, G. B.; Thomas, R. M.; Vacek, E. P.; Veale, C. A.; Tuthill, P. A.; Warner, P.; Williams, J. C.; Wolanin, D. J.; Woolson, S. A. Design of orally active, nonpeptidic inhititors of human leukocyte elastase. *J. Med. Chem.* **1994**, *37*, 1259−1261.

(8) (a) Reiner, J. E.; Siev, D. V.; Araldi, G.-L.; Cui, J. J.; Ho, J. Z.; Reddy, K. M.; Mamedova, L.; Vu, P. H.; Lee, K.-S. S.; Minami, N. K.; Gibson, T. S.; Anderson, S. M.; Bradbury, A. E.; Nolan, T. G.; Semple, J. E. Noncovalent thrombin inhibitors featuring P_3-heterocycles with P_1-monocylic arginine surrogates. *Bioorg. Med. Chem. Lett.* **2002**, *12*, 1203−1208. (b) Sanderson, P. E. J.; Cutrona, K. J.; Dorsey, B. D.; Dyer, D. L.; Mcdonough, C. M.; Naylor-Olsen, A. M.; Chen, I. W.; Chen, Z.; Cook, J. J.; Gardell, S. J.; Krueger, J. A.; Lewis, S. D.; Lin, J. H.; Lucas, B. J., Jr.; Lyle, E. A.; Lynch, J. J., Jr.; Stranieri, M. T.; Vastag, K.; Shafer, J. A.; Vacca, J. P. L-374,087, an efficacious, orally bioavailable, pyridinone acetamide thrombin inhibitor. *Bioorg. Med. Chem. Lett.* **1998**, *8*, 817−822. (c) Isaacs, R. C. A.; Cutrona, K. J.; Newton, L.; Sanderson, P. E. J.; Solinsky, M. G.; Baskin, E. P.; Chen, I. W.; Cooper, C. M.; Cook, J. J.; Gardell, S. J.; Lewis, S. D.; Lucas, R. J., Jr.; Lyle, E. A.; Lynch, J. J., Jr.; Naylor-Olsen, A. M.; Stranieri, M. T.; Vastag, K.; Vacca, J. P. C6 Modification of the pyridinone core of thrombin inhibitor L-374,087 as a means of enhancing it oral absotprion. *Bioorg. Med. Chem. Lett.* **1998**, *8*, 1719−1724. (d) Sanderson, P. E. J.; Lyle, T. A.; Cutrona, K. J.; Dyer, D. L.; Dorsey, B. D.; McDonough, C. M.; Naylor-Olsen, A. M.; Chen, I. W.; Chen, Z.; Cook, J. J.; Cooper, C. M.; Gardell, S. J.; Hare, T. R.; Krueger, J. A.; Lewis, S. D.; Lin, J. H.; Lucas, B. J., Jr.; Lyle, E. A.; Lynch, J. J.; Stranieri, M. T.; Vastag, K.; Yan, Y.; Shafer, J. A.; Vacca, J. P. Efficacious, orally bioavailable thrombin inhibitors based on 3-aminopyridinone or 3-aminopyrazinone acetamide peptidomimetic templates. *J. Med. Chem.* **1998**, *41*, 4466−4474. (e) Sanderson, P. E. J.; Dyer, D. L.; Naylor-Olsen, A. M.; Vacca, J. P.; Gardell, S. J.; Lewis, S. D.; Lucas, B. J., Jr.; Lyle, E. A.; Lynch, J. J., Jr.; Mulichak, A. M. L-373,890, An achiral, noncovalent, subnanomolar thrombin inhibitor. *Bioorg. Med. Chem. Lett.* **1997**, *7*, 1497−1500. (f) Tamura, S. Y.; Semple, J. E.; Reiner, J. E.; Goldman, E. A.; Brunck, T. K.; Lim-Wilby, M. S.; Carpenter, S. H.; Rote, W. E.; Oldeshulte, G. L.; Richard, B. M.; Nutt, R. F.; Ripka, W. C. Design and synthesis of a novel class of thrombin inhibitors incorporating heterocyclic dipeptide surrogates. *Bioorg. Med. Chem. Lett.* **1997**, *7*, 1543−1548.

(9) Duffy, J. L.; Laali, K. K. Aprotic Nitration ($NO_2^+BF_4^-$) of 2-halo- and 2,6-dihalopyridines and transfer-nitration chemistry of their N-nitropyridinium cations. *J. Org. Chem.* **1991**, *56*, 3006−3009.

(10) Barney, C. L.; Huber, E. W.; McCarthy, J. R. A convenient synthesis of hindered amines α-trifluoromethylamines from ketones. *Tetrahedron Lett.* **1990**, *31*, 5547−5550.

(11) Parlow, J. J.; South, M. S. Synthesis of 2-Pyridones as Tissue Factor VIIa inhibitors. *Tetrahedron* **2003**, *59*, 7695−7701.

JM0301686